Jurnal Ilmu Fisika
Vol. 18, No. 1, March 2026, pp. 14–24
ISSN: 1979-4657 (Print); 2614-7386 (Online)
https://doi.org/ 10.25077/jif.18.1.14-24.2026

Equilibrium Points and Periodic Orbits of Artificial Satellite Adjacent to an Oblate and Rotating Asteroid

Fauzia La Fatsa[1], Budi Dermawan[2]

[1] Master Program in Astronomy, Faculty of Mathematics and Natural Sciences, Institut Teknologi Bandung, Bandung, 40132, Indonesia
[2] Astronomy Research Group & Bosscha Observatory, Faculty of Mathematics and Natural Sciences, and University Center of Excellence for Space Science, Technology and Innovation, Institut Teknologi Bandung, Bandung, 40132, Indonesia

Article Info

Article History:

Received June 24, 2025
Revised September 08, 2025
Accepted September 21, 2025
Published online October 05, 2025

Keywords:

Asteroids
Artificial Satellites
Equilibrium Points
Periodic Orbits
Potentials

Corresponding Author:

Fauzia La Fatsa,
Email: fauzia.lf155@gmail.com

ABSTRACT

Asteroids have various shapes (mostly irregular) and physical characteristics. Space missions to asteroids are becoming frequent, and a global mapping scheme is applied to collect the asteroids' physical properties. Depending on the mission purposes, the mapping scheme can encircle the whole asteroid's body or utilize the asteroid's equilibrium points for the least energy consumption. Furthermore, it is essential to construct optimal trajectories to maximize the coverage and science results. Thus, an efficient mission can be achieved by devoting periodic orbits of artificial satellites around the equilibria. This study aims to construct periodic orbits related to the equilibria of an oblate shape and rotating asteroid, under the influences of gravitational and rotational potentials. Equations of motion of the satellite affected by the potentials are formulated in the Cartesian coordinate system. By acquiring mutual zero accelerations (first derivative of the potentials with respect to all directions), the equilibria are then obtained. Adjacent to the asteroid, four equilibria were revealed, and analysis of their stability showed that all of them are unstable. Despite this, some periodic orbits centered at the respective equilibria were successfully constructed using some arbitrary parameters (harmonics) that affect the coverage area for mapping the asteroid.

1. INTRODUCTION

Asteroids are celestial objects that are unique in their shapes, mostly irregular. Asteroids rotate with periods ranging from several minutes (smaller sizes) to hours (larger sizes). The surface of an asteroid generally has uneven features, such as various pits and craters. In addition to their physical differences, asteroids vary in their orbits around the Sun. Most known asteroids reside between the orbits of Mars and Jupiter, called the Main Belt. The other main population is Near-Earth Asteroids (NEAs), whose orbits are close to the Earth's orbit. A population part of the NEAs is Potentially Hazardous Asteroids (PHAs). The PHAs are asteroids that endanger Earth due to their potential to collide with Earth. The presence of PHAs encourages us to delve deeper into them, especially the knowledge of their orbits and physical characteristics.

Besides conducting astronomical observations on Earth, the accurate physical properties of asteroids can be revealed by sending artificial satellites or probes to the target asteroid. A mission to asteroids includes designing trajectories for mapping the asteroid's surface or even landing the probe to

take samples and return to Earth. The last approach is the most difficult scheme, and before doing so, the asteroid should be mapped by maneuvering the satellite near the asteroid to provide detailed spatial information. The maneuvers can be efficient by constructing periodic orbits concerning the asteroid's equilibrium points, which are revealed from its gravitational and rotational potentials.

Periodic orbits of the artificial satellite have many forms.Yu & Baoyin (2012) constructed 29 trajectories of periodic orbits from well-known asteroids with the corresponding physical parameters, such as asteroid Kleopatra. Many approaches are implemented for constructing periodic orbits, such as Chanut et al. (2015), Jiang & Baoyin (2016), and Jiang & Liu (2019), which uses an asteroid's shape model as multiple and single polyhedron objects. Recently, Abad et al. (2024) modelled asteroid (216) Kleopatra with a dipole-segment, which was improved with a 4th order polynomial density profile by Huda et al. (2025). Furthermore, Seitz et al. (2023) employ mathematical harmonic expansions to model the asteroid's shape, while Aksenov & Bober (2018) and Mota & Rocco (2019) use exponential and finite Fourier series to construct periodic orbits. On the other hand, some works related to modeling the potentials are worth noticing, i.e., Santos et al. (2017), Shi et al. (2018), and Hilst (2004).

In addition to these works, recent studies have further emphasized the role of equilibrium points and periodic orbits in small-body dynamics. Huda et al. (2023) derived the equilibrium points of the Sun-Haumea system in the modified circular restricted three-body problem. Jiang et al. (2014) analyzed equilibrium points in rotating asteroid potentials and found that while they are typically unstable, they provide essential anchors for constructing orbit families. Liu et al. (2022) extended this analysis to asteroid Minerva, confirming that all equilibria identified were unstable, yet still usable as reference centers for periodic trajectories. Observational evidence, such as the elongated shape and triplicity of asteroid (216) Kleopatra (Descamps et al., 2011), reinforces the necessity of realistic shape modeling when investigating gravitational environments. From a mission-design perspective, Li et al. (2019) reviewed advances in orbital dynamics and control around asteroids, while Takahashi & Scheeres (2021) demonstrated how periodic orbits can enable autonomous spacecraft exploration near NEAs. Related investigations on periodic orbit stability around specific asteroids, such as Eros and other irregular bodies (Ni et al. 2016; Scheeres 2016), further highlights the importance of combining gravitational modeling with orbital analysis. These insights collectively support the approach of this study.

The purpose of this study is to construct periodic orbits concerning the equilibria of an oblate shape and rotating asteroid, under the influences of gravitational and rotational potentials. In general, the irregular shape of an asteroid can be approximated by a triaxial shape. In this work, the triaxial shape is reduced to an oblate shape, since many asteroids' shapes show nearly a circular equator. The existence of the asteroid's equilibrium points is first derived regarding an oblate shape and a rotating asteroid. The points are then utilized as references for the periodic orbits under the influence of the potentials. The amplitudes of the periodic orbits can be adapted for the scientific purposes of the mission. We assumed the artificial satellite had arrived close to the target asteroid after a long passage in interplanetary space since its launch. The passage is beyond the scope of this study.

2. METHOD

We focus on constructing trajectories of an artificial satellite adjacent to the target asteroid. Along with the trajectories, solar gravitational perturbation has no such difference in acting on the asteroid and the satellite. The asteroid is substantially far from any other massive objects, such as planets. The equations of motion for such a case have been provided elsewhere, e.g., Scheeres et al. (1996) and Aljbaae et al. (2017). The formulation of the equations of motion of the satellite in a rotating Cartesian coordinate system (x-y-z) under the influence of an effective potential $V(x,y,z)$ is as follows.

$$\ddot{x} - 2\omega\dot{y} - \omega^2 x = \frac{\partial V}{\partial x},$$

$$\ddot{y} + 2\omega\dot{x} - \omega^2 y = \frac{\partial V}{\partial y}, \tag{1}$$

$$\ddot{z} = \frac{\partial V}{\partial z},$$

where a dot and double dots are respectively the first and second derivatives with respect to time, ω is the asteroid's spin rate, and V comprises gravitational and rotational potentials. The asteroid rotates around its short principal axis (z-axis).

The gravitational potential is derived by considering an oblate geometrical shape. Following Hilst (2004), the gravitational potential V_g of an oblate body of mass M and the universal gravitational constant G can be written as MacCullagh's formula.

$$V_g(r, \Lambda) = -\frac{GM}{r} - \frac{G}{r^3}(I_C - I_A)\left(\frac{3}{2}\sin^2\Lambda - \frac{1}{2}\right), \quad (2)$$

where r is the distance vector from the center of mass of the model asteroid to the satellite around it, Λ is the latitude of an oblate body, and I_A and I_C are the moments of inertia with respect to the x- and y-axis, respectively. The asteroid's non-spherical shape is expressed mathematically by the Legendre polynomial expansion of order two, which is equivalent to the zonal spherical harmonics. The oblate shape implies the equatorial radius (a) is larger than the polar one, and the oblateness can be conveyed in terms of the coefficient of ellipticity of the body (J_2). For a general axisymmetric mass distribution, the dimensionless coefficient J_2 is expressed as

$$J_2 = \frac{(I_C - I_A)}{MR^2}, \quad (3)$$

R is the mean radius of the body. In this work, we assumed the value of the asteroid's J_2 is roughly the same as the Earth's ($1.08262668 \times 10^{-3}$). Nevertheless, we specify the role of the J_2 in Section 3.

Because the asteroid rotates around the z-axis, the rotational potential (V_r) is

$$V_r = -\frac{1}{2}a^2\omega^2. \quad (4)$$

Hence, the effective potential converges at the asteroid's equator and becomes

$$V = -\frac{GM}{a} - \frac{GM}{2a}J_2 - \frac{1}{2}a^2\omega^2 = -\frac{1}{2}\frac{GM(2+J_2)}{\sqrt{x^2+y^2}} - \frac{1}{2}(x^2+y^2)\omega^2. \quad (5)$$

The first and second terms on the right-hand side represent the gravitational potential, with the second term standing for the oblateness representation, and the last term is the rotational potential.

We chose two asteroids, Minerva and 2008 EV5, to apply the scheme and generate periodic orbits around their respective equilibrium points. Asteroids' physical properties related to this study are given in Table 1. Asteroid Minerva belongs to the Main Belt, while asteroid 2008 EV5 represents the NEAs population. Dimensions of the asteroids are suitable for seizing the oblate geometrical shape. Masses of the asteroids can be obtained by the standard relation: volume × density (ρ).

Table 1. Physical parameters of asteroids Minerva and 2008 EV5.

Asteroid	Dimension ($x \times y \times z$) [km]	Density [kg m^{-3}]	Period [h]	Ref.
Minerva	183 × 164 × 144	1750	5.982	Liu et al. (2022)
2008 EV5	0.415 × 0.410 × 0.385	3000	3.725	Busch et al. (2011)

2.1 Equilibrium Points

Equilibrium points are the points where the net accelerations in all directions are zero. Hence, the points have no motion relative to the reference coordinate system. Depending on its physical properties, several equilibrium points may exist inside and outside of an asteroid body (Liu et al., 2022). Constructing a satellite's trajectory regarding the equilibrium points below an asteroid's surface is difficult and complex. In this work, we use the outside equilibrium points as the epicenters of periodic orbits.

The equilibrium points can be revealed by applying partial derivatives of the effective potential (Equation 3). The partial derivatives represent the accelerations or the forces acting along all spatial directions in the coordinate system. Zero values of the derivatives imply that the net accelerations equal zero in every direction, and thus, no motion occurs at the equilibrium points. Since the asteroids rotate

in their respective z-direction, the partial derivatives are applied in the x and y directions. The results are given in Equation 6 and advancing them to zero in Equation 7,

$$\frac{\partial V}{\partial x} = \frac{GM(2+J_2)x}{2(x^2+y^2)^{3/2}} - x\omega^2 \; ; \qquad \frac{\partial V}{\partial y} = \frac{GM(2+J_2)y}{2(x^2+y^2)^{3/2}} - y\omega^2. \tag{6}$$

$$\frac{\partial V}{\partial x} = \frac{\partial V}{\partial y} = 0, \tag{7}$$

and employing a mesh grid in the x and y directions reveals the zero accelerations around the asteroids. Because an equilibrium point should satisfy zero accelerations for both the x and y directions, we manage contours of zero accelerations to find their intersections, which represent the equilibrium points (E). Because our oblate model is symmetric, it is expected that several equilibrium points may reside symmetrically in the vicinity of the asteroids.

2.2 Stability of the Equilibrium Points

Whether the state of the equilibrium points is stable or unstable, a steady satellite trajectory, i.e., without consuming much fuel, around the equilibrium points can still be constructed. Choosing the appropriate initial values can optimize the steadiness of the satellite trajectory. To examine the stability of the equilibria, the equations of motion relative to the equilibria are expanded linearly with small variations. A common expansion scheme used in this case is the Taylor expansion (e.g., Jiang et al. 2014; Jiang & Baoyin 2016). Since this scheme evaluates the linear stability, it takes only the linear part of the expansion. Thus, the equations of motion around the equilibrium point are linearised, and the characteristic equation of motion is then derived. The roots (λ) of the characteristic equation are explored to investigate the state of stability. Jiang et al. (2014) describe the steps of the scheme.

The linearised equations of motion relative to the equilibrium point can be expressed in the following form,

$$\begin{gathered} \ddot{x} - 2\omega\dot{y} + V_{xx}x + V_{xy}y = 0, \\ \ddot{y} + 2\omega\dot{x} + V_{xy}x + V_{yy}y = 0, \\ \ddot{z} = 0. \end{gathered} \tag{8}$$

Because the asteroid rotates on the z-axis, the equilibrium points lie in the x-y plane. The characteristic equation is a sextic equation for λ,

$$\lambda^6 + \left(V_{xx} + V_{yy} + 4\omega^2\right)\lambda^4 + \left(V_{xx}V_{yy} - V_{xy}^2\right)\lambda^2 = 0. \tag{9}$$

The subscripts denote partial derivatives with respect to the coordinate system, and the sequence is changeable, i.e., $V_{xy} = V_{yx}$.

There are two states of equilibrium points, i.e., stable and unstable. A stable equilibrium point implies a satellite's trajectory tracks in its lowest energy dissipation, and the trajectory may have small variations under stability. On the other hand, when the trajectory encircles the unstable equilibrium point, it may have small variations. More efforts should be made to keep the satellite stably around the points. Thus, both states are a matter of efficiency. Nevertheless, regardless of the state of stability of the equilibrium points, periodic orbits can be constructed encircling the points for both states.

To evaluate the stability of the equilibrium points, the second partial derivatives of the effective potential in Equation 9 are utilized. Equation 10 shows the derivatives, and the stability states can be determined by evaluating the roots λ.

$$\begin{gathered} V_{xx} = \frac{\partial^2 V}{\partial x^2} = \frac{G(2+J_2)M(2x^2-y^2)}{2(x^2+y^2)^{5/2}} - \omega^2, \\ V_{yy} = \frac{\partial^2 V}{\partial y^2} = \frac{G(2+J_2)M(x^2-2y^2)}{2(x^2+y^2)^{5/2}} - \omega^2, \\ V_{xy} = \frac{\partial^2 V}{\partial xy} = \frac{3G(2+J_2)Mxy}{2(x^2+y^2)^{5/2}}. \end{gathered} \tag{10}$$

The characteristic roots λ resemble the eigenvalues of Equation 9, and imply the condition of the forthcoming trajectories. The roots in terms of λ^2 can be obtained from Equation 11,

$$\lambda_{1,2}^2 = \frac{-\beta \pm \sqrt{\beta^2 - 4\alpha\gamma}}{2\alpha}, \tag{11}$$

with $\alpha = 1, \beta = V_{xx} + V_{yy} + 4\omega^2$, and $\gamma = V_{xx}V_{yy} - V_{xy}^2$. Solution of Equation 11, the λs, can be real, complex, or pure imaginary values. Moreover, the solutions of Equation 9 are in the form of $e^{\lambda t}$ along with the time t. The state of stability can only be achieved if all the λs are pure imaginaries, or in the trivial solution, this will occur when $V_{xx} = V_{yy} = V_{xy} = 0$. This means that the trajectory encircling the equilibrium points will be enclosed within the sine and cosine forms, while otherwise, the trajectory will be divergent.

2.3 Periodic Orbits

In this study, we implemented two straightforward formulations of periodic orbits, which are described by McInnes (2009) and Mota & Rocco (2019). Both formulations provide some arbitrary parameters that can be attuned to the purpose of the satellite mission. This is important since many periodic orbits can be constructed to optimize the scientific results of the mission.

One among the solutions of periodic orbits encircling the equilibrium point can follow a Lissajous path (McInnes (2009)), which is given in Equation 12. The periodic orbit or trajectory of the satellite in the Cartesian coordinates as a function of t obeys,

$$\begin{aligned} x(t) &= P_1 \cos(f_\lambda t) + P_2 \sin(f_\lambda t), \\ y(t) &= -\kappa P_1 \sin(f_\lambda t) + P_2 \cos(f_\lambda t), \\ z(t) &= Q_1 \cos(f_v t) + Q_2 \sin(f_v t), \end{aligned} \tag{12}$$

where f_λ and f_v are the in-plane and out-of-plane frequencies, P_1, P_2, Q_1, Q_2 are arbitrary parameters, and κ is the correspondence coefficient in the x and y directions. Note that the constructing trajectory can stretch to all directions, including the z-direction. The starting point is located at $t = 0$, and hence, the arbitrary parameters can be adjusted so that the trajectory meets the purposes of the mission.

Another solution is described by Mota & Rocco (2019), which is one among the general solutions given by Jiang et al. (2014). Formulation of periodic orbits in this solution is more complex than that of the previous one. Many arbitrary parameters are involved, and a more detailed trajectory can be yielded. Equation 13 shows the formulation,

$$\begin{aligned} x(t) &= A_{x1}e^{\rho_1 t} + B_{x1}e^{-\rho_1 t} + \sum_{k=1}^{3}[C_{xk}\cos(\theta_k t) + S_{xk}\sin(\theta_k t)], \\ y(t) &= A_{y1}e^{\rho_1 t} + B_{y1}e^{-\rho_1 t} + \textstyle\sum_{k=1}^{3}\big[C_{yk}\cos(\theta_k t) + S_{yk}\sin(\theta_k t)\big], \\ z(t) &= A_{z1}e^{\rho_1 t} + B_{z1}e^{-\rho_1 t} + \sum_{k=1}^{3}[C_{zk}\cos(\theta_k t) + S_{zk}\sin(\theta_k t)], \end{aligned} \tag{13}$$

with sets of A, B, C, and S are arbitrary parameters as well as ρ_1 and a set of θ. With many arbitrary parameters, it opens an opportunity to produce various trajectories, including managing to hover the satellite close to the asteroid's surface. Like the previous one, the starting point of the trajectory is located at $t = 0$.

Table 2. Coordinates of the equilibrium points of asteroids Minerva and 2008 EV5.

Asteroid	E1 [km]	E2 [km]	E3 [km]	E4 [km]
Minerva	(138.165366, 0)	(–138.165366, 0)	(0, 138.165366)	(0, –138.165366)
2008 EV5	(0.3122193, 0)	(– 0.3122193, 0)	(0, 0.3122193)	(0, – 0.3122193)

3. RESULTS AND DISCUSSION

3.1 The Equilibrium Points and Periodic Orbits

We apply Equations 6 and 7 with the data in Table 1 to find all the equilibrium points. Figure 1 shows the locations of all the points for asteroids Minerva and 2008 EV5. There are two contours of zero accelerations, i.e., the red for $\partial V/\partial x = 0$ and the blue for $\partial V/\partial y = 0$, yielding four intersections,

which are all the equilibrium points (E). All the points are outside the respective asteroids and symmetric to them. This symmetry is simply because of the symmetrical geometry model of the oblate shapes. Locations of the equilibrium points are given in Table 2.

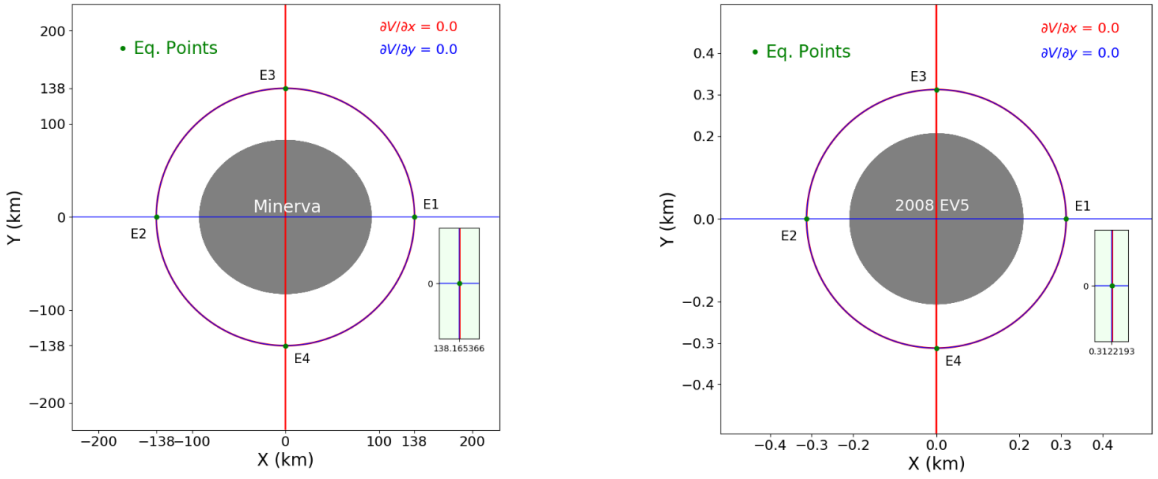

(a) (b)

Figure 1. Equilibrium points (E) of asteroids (a) Minerva and (b) 2008 EV5. Cross-sections of the asteroids are illustrated with grey areas. Inset plots show the intersections for E1 of Minerva and 2008 EV5, respectively.

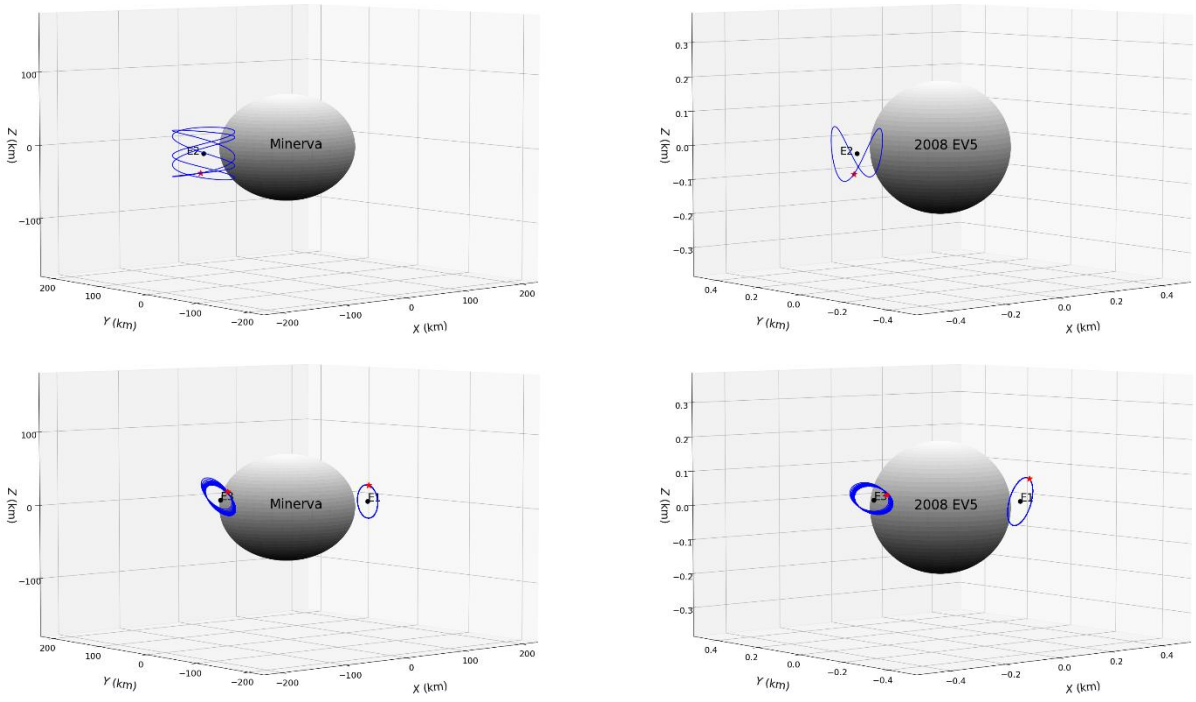

(a) (b)

Figure 2. Examples of periodic orbits (blue) for asteroids (a) Minerva and (b) 2008 EV5. The trajectories are generated from Equation 12 (top panels) and Equation 13 (bottom panels).

It is evident from Figure 1 that all the equilibrium points are located significantly far from the surfaces of the respective asteroids. For Minerva, the points are situated approximately 40% of its radius above the surface. The coordinates of the points are found to be a small difference from those described

in Liu et al. (2022) . This is because Liu et al. (2022) used a different geometric model, i.e., a polyhedral shape. Meanwhile, the equilibrium points of 2008 EV5 are situated approximately 50% of its radius above the surface. We reveal the equilibrium points of 2008 EV5, which were not provided by Busch et al. (2011).

Given these conditions, it is safe to plan some maneuvers for the satellite due to the ample spatial range. Following Jiang et al. (2014), we investigate various values of the arbitrary parameters in Equations 12 and 13 to generate periodic orbits near each of the asteroids. In Figure 2, we present two examples of the constructed periodic orbits for each of the asteroids, encircling the equilibrium points. The top panels are yielded from Equation 12 for E2, while the bottom panels are from Equation 13 for E1 and E3. In these examples, the minimum distances of the trajectories to the asteroid's surfaces are no less than 14.3 km for Minerva (left panels) and 0.02 km for 2008 EV5 (right panels).

In this study, we further investigate the role of the rotation period of the asteroids in constructing the trajectory. It is known that asteroids have a wide range of rotation periods, from about several minutes for small sizes to some hours for larger sizes. However, there are many asteroids for which there is no available information about their rotation periods. Moreover, some recent asteroid missions, such as Hera to asteroid Didymos (size of 780 m), Brokkr-2 to asteroid 2022 OB5 (size of 100 m), and Tianwen-2 to asteroid Kamo'oalewa (size of 40 – 100 km), target small asteroids.

Very recently, Fu & Soldini (2025) studied the equilibrium point evolution caused by the YORP (Yarkovsky-O'Keefe-Raszievskii-Paddack) thermal effect acting on asteroid 2000 PH5. The asteroid exhibits a rotational acceleration of 7.7×10^{-8} rad d^{-2} (Zegmott et al. (2021)) that can speed up the spin rate of the asteroid over time. The next paragraph provides insights into constructing satellite trajectories near fast-rotating asteroids.

Table 3. Coordinates of the equilibrium points of fast-rotating asteroids Minerva and 2008 EV5.

Asteroid	E1 [km]	E2 [km]	E3 [km]	E4 [km]
Minerva	(105.334, 0)	(–105.334, 0)	(0, 105.334)	(0, –105.334)
2008 EV5	(0.2535, 0)	(– 0.2535, 0)	(0, 0.2535)	(0, – 0.2535)

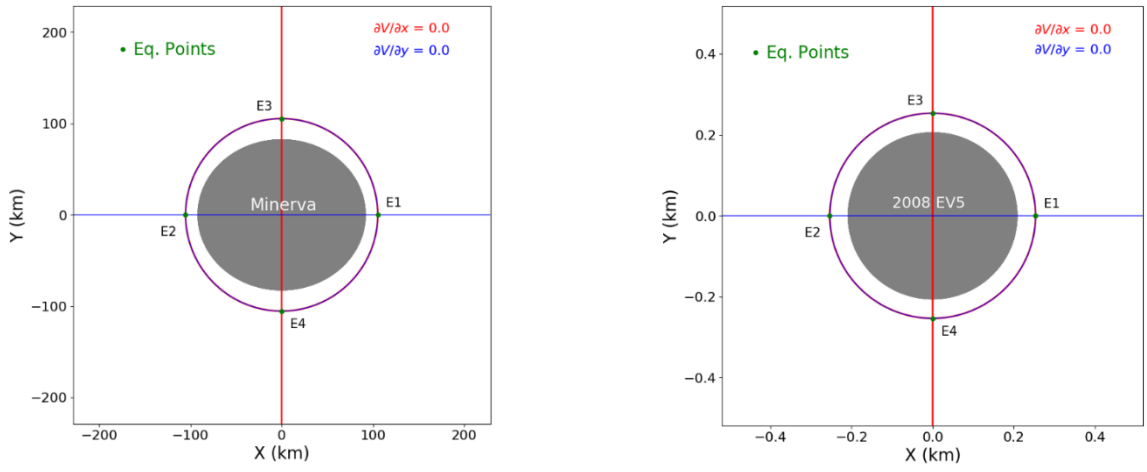

(a) (b)

Figure 3. Equilibrium points (E) of fast-rotating asteroids (a) Minerva with a rotation period of 3.982 h and (b) 2008 EV5 with a rotation period of 2.725 h.

We speed up the rotation periods of Minerva by 2 h and that of 2008 EV5 by 1 h. Hence, the rotation periods of fast rotators Minerva and 2008 EV5, respectively, become 3.982 h and 2.725 h. With these attempts, the equilibrium points of the asteroids move closer to the asteroids' surfaces (Table 3 and Figure 3). The equilibrium points can even reside inside the asteroids' bodies if the rotation periods are sped up. This condition is in accordance with some of the results by Liu et al. (2022) for Minerva. Moreover, by using ratios of parameters applied to trajectories in Figure 2, trajectories of satellites near

the fast-rotating asteroids are given in Figure 4. For these fast rotators, the minimum distances of the trajectories to the asteroids' surfaces become only 1.70 km for Minerva and 0.028 km (= 28 m) for 2008 EV5. Although ratios of parameters are somewhat arbitrary, these imply that a scenario of the satellite trajectories should be carefully constructed because the satellite can descend very close to the asteroid surfaces. Indeed, this also depends on the mission goals.

3.2 Stability Analyses of the Equilibrium Points

After utilizing the contours of zero accelerations (Equation 7) to Equation 6, the equilibrium points are yielded. Here, we provide the results of the linear stability analyses of the equilibrium points in Table 2 and those in Table 3 for the examples of fast-rotating asteroids.

The characteristic equation in Equation 9 is the primary expression to investigate the linear stability of the equilibrium points. To do that, we appointed each of the locations of the obtained equilibrium points listed in Tables 2 and 3 to Equation 10, and sought all roots of Equation 11. An equilibrium point will be stable if and only if all of the roots are pure imaginary. After putting all the obtained equilibrium points, we finally acquire that all of the roots are sets of real and/or complex numbers, and there is no pure set of imaginary numbers. We also attempted to explore several other values of the rotation periods for slow rotators (e.g., 10.982 h) to get the same results. Thus, this implies the unstable states of all the obtained equilibrium points, including the fast and slow rotators. This tendency is also found by Jiang et al. (2014) and Liu et al. (2022).

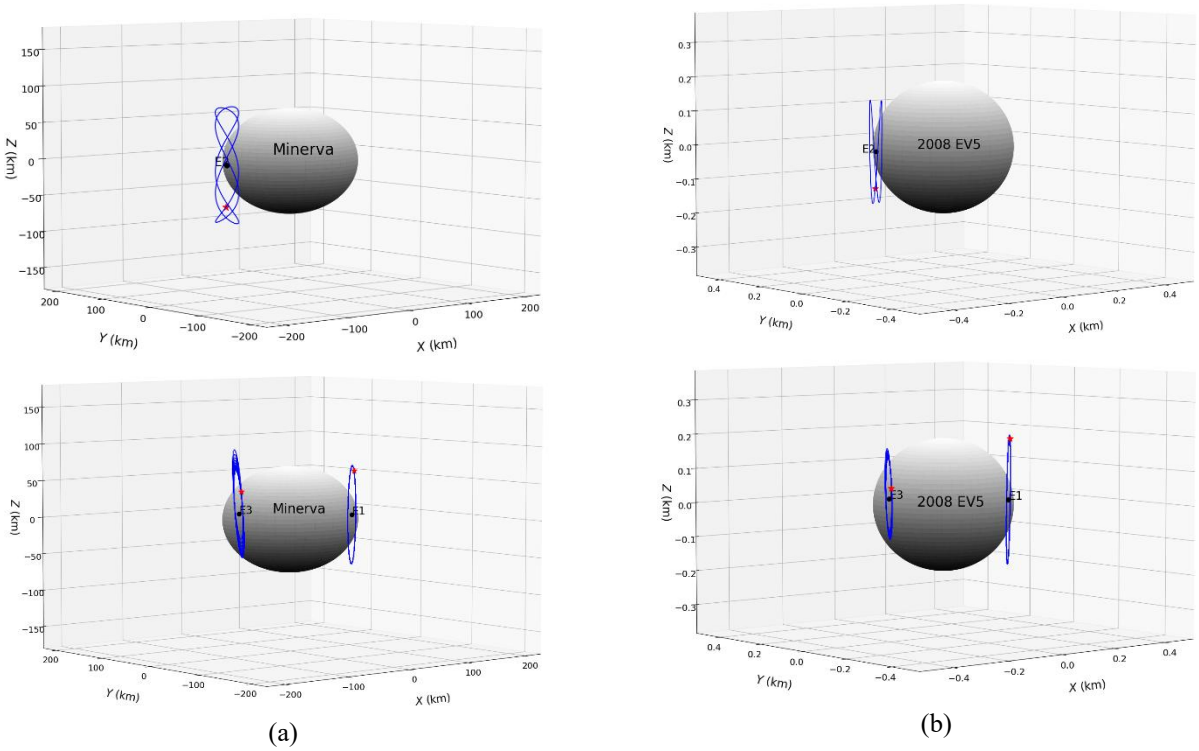

Figure 4. Periodic orbits (blue) of the satellites regarding the equilibrium points for fast-rotating asteroids (a) Minerva and (b) 2008 EV5 with ratios of parameters as those in Figure 2.

We further examine the roles of the asteroid's mass and the coefficient J_2 in influencing the linear stability of the equilibrium points. We conduct tests by varying these parameters around the nominal values of Minerva. For the mass, we used factors of 0.5 and 2 of the nominal value 3.3603×10^{18} kg. We also varied the J_2 by factors of 0.1 and 10 times the Earth's. In all cases, all the equilibrium points remain unstable, with naturally no change in the state of the roots (sets of real and/or complex numbers). Santos et al. (2017) found the same occurrence for asteroid 2001 SN263.

These findings confirm that variations in the rotation period, mass, and J_2 do not entirely affect the stability states of the equilibrium points within the tested ranges. However, it is noted that smaller mass and faster rotation may cause the equilibrium points to shift closer to, or even below, the asteroid's surface, which has implications for trajectory design and mission safety.

3.3 Discussion

In this study, we intended to and concentrated on exploring the construction of periodic orbits, which are dominantly guided by arbitrary parameters. Despite the unstable states of all the equilibrium points, there are enough opportunities to construct steady trajectories of the satellite by choosing appropriate initial values, as described in Jiang et al. (2014). In addition to the work by Jiang et al. (2014), here we put the constraints of permissible distances from the asteroid's surfaces (see Section 3.1) in assembling the parameters of the formulas in Equations 12 and 13. Instability in the equilibria does not mean satellite trajectories are always unstable, except that the steady trajectories do not move under the lowest energy environment. Rigorous schemes to calculate values of and relations among the parameters are given elsewhere, e.g., Liu et al. (2022), and this can be adapted to some detailed purposes of the mission.

Table 4. Locations of the equilibrium points adjacent to Minerva with increasing J_2 values.

J_2 values	E1 [km]	E2 [km]	E3 [km]	E4 [km]
1 × Earth's J_2	(138.165366, 0)	(–138.165366, 0)	(0, 138.165366)	(0, –138.165366)
5 × Earth's J_2	(138.264961, 0)	(–138.264961, 0)	(0, 138.264961)	(0, –138.264961)
10 × Earth's J_2	(138.389254, 0)	(–138.389254, 0)	(0, 138.389254)	(0, – 138.389254)

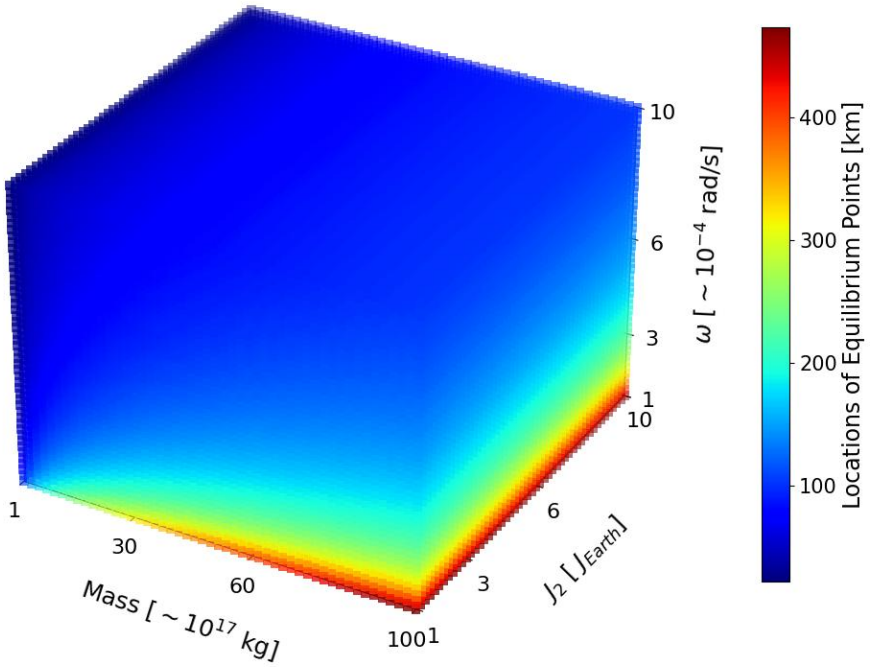

Figure 5. Overall effects of variations (ω, J_2, and M) in the locations of the equilibrium points adjacent to the asteroid. Colors from blue to red represent the farther locations of the equilibrium points.

We mentioned in Section 3.1 that fast-rotating asteroids tend to pull in the equilibrium points towards the asteroid's body. We show this tendency by comparing results in Table 2 (or Figure 1) and Table 3 (or Figure 3). On the other hand, the slow-rotating ones push out the equilibria, which is the same trend (although very small) as the role of the J_2. Although we employ the J_2 value of the Earth (1.0826×10^{-3}) as an assumption, we investigate up to one order of magnitude larger values to finally

reveal small displacements of the resulting equilibria locations. Table 4 shows the locations of the equilibria with increasing values (5 and 10 times the Earth's J_2). This result upholds the role of the J_2 described in Hilst (2004) and Santos et al. (2017).

The differences in the equilibrium point locations due to increasing J_2 values are very small (up to 0.2%) but measurable. We notice the displacements are about 124 meters and 224 meters for 5 J_2 and 10 J_2, respectively. This effect remains minor compared to the dominant influence of the rotation period listed in Table 3. It is reasonable since the effective potential in Equation 3, emphasizing the bracket ($2 + J_2$), shows that the coefficient J_2 (1.0826×10^{-3}) is indeed very small relative to the value of 2.

We obtained the same trend with the increasing mass of the asteroid. The more massive the asteroid, the more distant the equilibria. This supports the basic concept provided in Hilst (2004). We find that the displacement of the equilibria because of the increasing mass by two orders of magnitude is comparable with that of the rotation period. Figure 5 illustrates the overall effects of the whole variations: ω, J_2, and M, on the locations of the equilibria. We use Minerva's physical properties as a reference. Figure 5 shows that a faster asteroid's spin rate will pull in the locations of the equilibria straightforwardly, whereas the increasing asteroid's mass tends to push out the equilibria deviously. On the other hand, it is also clear that increasing values of J_2 have no significant evidence of displacement of the equilibria.

It is worth noting that when the equilibrium points are located close to the asteroid surface, it is preferable to construct the trajectories to cope with higher latitudes (higher amplitudes in the z-direction). Our investigations are forthright compared with the rigorous works by Yu & Baoyin (2012) and Jiang & Baoyin (2016). Because of the limited height of the equilibrium points from the surface, it is unnecessary to build large movements to the asteroid's center directions (whether the x- or y-directions depend on the location of the point E) to avoid the satellite crashing. We made these approaches, which are shown in Figure 4, where the trajectories have higher amplitudes in the z-direction.

4. CONCLUSION

We study the construction of periodic orbits epicentered at the equilibrium points adjacent to a Main Belt asteroid, Minerva, and a NEA 2008 EV5, with the physical properties in Table 1. Each of the asteroids has a gravitational potential of an oblate geometry shape and a rotational potential with a certain rotation period (spin rate) on the z-axis. Under these circumstances, four equilibrium points adjacent to the asteroids are obtained, and their locations are symmetric. All the equilibrium points are found to be unstable. Despite the unstable states of the equilibria, we successfully constructed some periodic orbits under the constraints of the parameters in Equations 12 and 13. Using the factual physical properties of the asteroids , trajectories of the periodic orbits have minimum distances from the asteroids' surfaces of no less than 14.3 km for Minerva and 0.02 km for 2008 EV5. We also analyze the effects of ω, J_2, and M variations on the displacements of the equilibria locations. Faster rotating asteroids tend to pull in the equilibrium points, in contrast with the increasing asteroid's mass. The increasing values of J_2 do not noticeably affect the displacement of the equilibria. The results of this study can benefit from enlarging reviews for constructing trajectories of satellites for doing sciences when mapping the target asteroids.

ACKNOWLEDGEMENT

FLF acknowledges the financial support of the GTA (Ganesha Talent Assistantship) during the Accelerated Undergraduate and Master Programs in Astronomy of ITB 2024 – 2025. BD and FLF are thankful to I. N. Huda for many fruitful discussions about this subject. FLF and BD acknowledge the reviewers for constructive comments that improve the quality of the article.

REFERENCE

Abad, A., Elipe, A., & Ferreira, A. F. S, (2024). Periodic orbits around the 216-Kleopatra asteroid modelled by a dipole-segment. *Advances in Space Research*, *74*(*11*), 5687-5697.

Aksenov, S. A., & Bober, S. A. (2018). Calculation and study of limited orbits around the L2 libration point of the Sun-Earth system. *Cosmic Research*, *56*(*2*), 144–150.

Aljbaae, S., Chanut, T. G., Carruba, V., Souchay, J., Prado, A. F., & Amarante, A. (2017). The dynamical environment of asteroid 21 Lutetia according to different internal models. *Monthly Notices of the Royal Astronomical Society*, *464*(*3*), 3552-3560.

Busch, M. W., Ostro, S. J., Benner, L. A., Brozovic, M., Giorgini, J. D., Jao, J. S., ... & Brisken, W. (2011). Radar observations and the shape of near-Earth asteroid 2008 EV5. *Icarus*, *212*(*2*), 649-660.

Chanut, T. G. G., Aljbaae, S., & Carruba, V. (2015). Mascon gravitation model using a shaped polyhedral source. *Monthly Notices of the Royal Astronomical Society*, *450*(*4*), 3742–3749.

Descamps, P., Marchis, F., Michalowski, T., Vachier, F., Colas, F., Berthier, J., … Birlan, M. (2011). Triplicity and physical characteristics of asteroid (216) Kleopatra. *Icarus, 211*(*2*), 1022–1033.

Fu, X. & Soldini, S. (2025). Equilibrium point evolution and the associated characteristic curves of an asteroid. *Monthly Notices of the Royal Astronomical Society*, *538*(*4*), 2245–2254.

Hilst, V. D. R. (2004). *Essentials of geophysics*. Open Course Ware. MIT. Retrieves from https://ocw.mit.edu/courses/12-201-essentials-of-geophysics-fall-2004/

Huda, I. N., Dermawan, B., Saputra, M. B. Sadikin, R. & Hidayat, T. (2023). Studying the equilibrium points of the modified circular restricted three-body problem: the case of Sun-Haumea system. *Research in Astronomy and Astrophysics*, *23*(*11*), #115025.

Huda, I. N., Haz, H. R. S., Dermawan, B., Abdurrazzaq, A., Rachmawati, R. N., & Kuntjoro, Y. D. (2025). Model of potential around natural elongated asteroid with 4th-order polynomial density profile and albedo effects. *Journal of the Astronautical Sciences*, *72*, *2*, 12 pp.

Jiang, Y., Baoyin, H., Li, J., & Li, H. (2014). Orbits and manifolds near the equilibrium points around a rotating asteroid. *Astrophysics and Space Science*, *349*(*1*), 83-106.

Jiang, Y., & Baoyin, H. (2016). Periodic orbit families in the gravitational field of irregular-shaped bodies. *The Astronomical Journal*, 152(5), 137.

Jiang, Y. & Liu, X. (2019). Equilibria and orbits around asteroid using the polyhedral model. *New Astronomy*, *69*(*1*), 8–20.

Li, X., Warier, R. R., Sanyal, A. K., & Qiao, D. (2019). Trajectory tracking near small bodies using only attitude control. *Journal of Guidance, Control, and Dynamics*, *42*(1), 109-122.

Liu, H., Jiang, Y., Lang, A., Wang, Y., Zou, X., Ping, J., & Cao, J. (2022). Analysis of the equilibrium points and orbits stability for the asteroid 93 Minerva. *Open Astronomy*, *31*(*1*), 375–389.

McInnes, A. I. (2009). *An introduction to libration point orbits*. Retrieved from https://api.semanticscholar.org/CorpusID:36564510

Mota, M. L., & Rocco, E. M. (2019). Equilibrium points stability analysis for the asteroid 21 Lutetia. In *Journal of Physics: Conference Series* (Vol. 1365, No. 1, p. 012007). IOP Publishing.

Ni, Y., Jiang, Y., & Baoyin, H. (2016). Multiple bifurcations in the periodic orbit around Eros. *Astrophysics and Space Science*, *361*(5), 170.

Santos, L. T., Prado, A. F. B. D. A., & Sanchez, D. M. (2017). Equilibrium points in the asteroid 2001 SN263. In *Journal of Physics: Conference Series* (Vol. 911, No. 1, p. 012023). IOP Publishing.

Scheeres, D. J. (2016). Orbital motion in strongly perturbed environments: applications to asteroid, comet and planetary satellite orbiters. Springer.

Scheeres, D. J., Ostro, S. J., Hudson, R. S., & Werner, R. A. (1996). Orbits close to asteroid 4769 Castalia. *Icarus*, *121*(*1*), 67–87.

Seitz, K., Heck, B., & Abd-Elmotaal, H. (2023). External gravitational field of a homogeneous ellipsoidal shell: A reference for testing gravity modelling software. *Journal of Geodesy*, *97*(*6*), 54.

Shi, Y., Wang, Y., & Xu, S. (2018). Equilibrium points and associated periodic orbits in the gravity of binary asteroid systems: (66391) 1999 KW4 as an example. *Celestial Mechanics and Dynamical Astronomy*, *130*, *32*.

Takahashi, S., & Scheeres, D. J. (2021). Autonomous Exploration of a Small Near-Earth Asteroid. Journal of Guidance, Control, and Dynamics, 44(4), 701–718.

Yu, Y., & Baoyin, H. (2012). Generating families of 3D periodic orbits about asteroids. *Monthly Notices of the Royal Astronomical Society*, *427*(*1*), 872–881.

Zegmott, T. J., Lowry, S. C., Rożek, A., Rozitis, B., Nolan, M. C., Howell, E. S., ... & Weissman, P. R. (2021). Detection of the YORP effect on the contact binary (68346) 2001 KZ66 from combined radar and optical observations. *Monthly Notices of the Royal Astronomical Society*, *507*(4), 4914-4932.